AGU PUBLICATIONS

JGR

Journal of Geophysical Research: Earth Surface

RESEARCH ARTICLE
10.1002/2016JF003946

Key Points:
- Tracers dispersed more rapidly over fully exposed bedrock than in reaches with partial sediment cover
- Tracers were least mobile in the upstream alluvial channel that controls supply to the bedrock segment
- Dispersion patterns are consistent with measured downstream changes in shear stress and estimated changes in threshold stress

Correspondence to:
R. I. Ferguson,
r.i.ferguson@durham.ac.uk

Citation:
Ferguson, R. I., B. P. Sharma, R. A. Hodge, R. J. Hardy, and J. Warburton (2017), Bed load tracer mobility in a mixed bedrock/alluvial channel, *J. Geophys. Res. Earth Surf.*, *122*, doi:10.1002/2016JF003946.

Received 4 MAY 2016
Accepted 4 MAR 2017
Accepted article online 8 MAR 2017

Bed load tracer mobility in a mixed bedrock/alluvial channel

R. I. Ferguson[1], B. P. Sharma[1], R. A. Hodge[1], R. J. Hardy[1], and J. Warburton[1]

[1]Department of Geography, Durham University, Durham, UK

Abstract The presence of bare or partially covered rock in an otherwise alluvial river implies a downstream change in transport capacity relative to supply. Field investigations of this change and what causes it are lacking. We used two sets of magnet-tagged tracer clasts to investigate bed load transport during the same sequence of floods in fully alluvial, bare rock, and partial-cover reaches of an upland stream. High-flow shear stresses in different reaches were calculated by using stage loggers. Tracers seeded in the upstream alluvial channel moved more slowly than elsewhere until the frontrunners reached bare rock and sped up. Tracers seeded on bare rock moved rapidly off it and accumulated just upstream from, and later in, a partial-cover zone with many boulders. The backwater effect of the boulder-rich zone is significant in reducing tracer mobility. Tracer movement over full or partial sediment cover was size selective but dispersion over bare rock was not. Along-channel changes in tracer mobility are interpreted in terms of measured differences in shear stress and estimated differences in threshold stress.

1. Introduction

Upland rivers often possess a streamwise alternation between fully alluvial segments and bedrock segments, where "bedrock" denotes a channel that cannot substantially widen, deepen, or migrate without eroding rock [*Whipple*, 2004; *Turowski et al*., 2008]. Bedrock segments are often associated with knickpoints and/or changes in lithology and almost always contain some sediment, ranging from isolated patches to an almost complete cover. It has long been recognized that exposed rock in a river bed implies that, averaged over time, the local bed-material transport capacity exceeds the supply of coarse sediment, but there have been few studies of how this situation arises. Understanding how coarse sediment passes through bedrock segments of otherwise alluvial streams is important because the geomorphological evolution of upland landscapes is usually limited by the rate at which rivers can incise into bedrock, and river incision into rock depends on the balance between the availability of sediment as an abrasive tool and the protective effect of a sediment cover [*Gilbert*, 1877].

Several models have been proposed for how sediment cover, tool availability, and long-term incision rate depend on water discharge and sediment supply in idealized situations [e.g., *Sklar and Dietrich*, 2004; *Turowski et al*., 2007; *Lague*, 2010; *Johnson*, 2014; *Zhang et al*., 2015]. These models involve assumptions about how sediment supply varies with discharge and how bed load transport capacity varies with shear stress. A modeling approach has the great advantage of linking short-term process considerations and long-term landscape evolution, but models remain speculative to some degree until their predictions and process assumptions have been tested against observations and measurements. Experiments in artificial channels have provided valuable constraints by showing how sediment cover and/or incision rate respond to imposed changes in sediment supply [e.g., *Finnegan et al*., 2007; *Chatanantavet and Parker*, 2008; *Johnson and Whipple*, 2010; *Inoue et al*., 2014; *Hodge and Hoey*, 2016], and the erosion of artificial "bedrock" by natural bed load has been investigated in a steep alluvial stream [*Beer et al*., 2015].

Fewer studies have been made of bed load transport as a freely adjustable part of the bedrock channel system. The most practical approach to studying it in the field is to use tracer stones. *Goode and Wohl* [2010] observed size-selective tracer dispersion where bedrock ribs were parallel to the flow, but lower mobility and unselective transport where ribs were transverse or oblique. *Hodge et al*. [2011] found unselective transport in a bedrock channel with 20% sediment cover and a higher virtual velocity (annual travel distance divided by duration of competent flow) than in two previously studied streams with 80% and 100% sediment cover. *Phillips and Jerolmack* [2014] showed that tracer dispersion in a coarse alluvial channel and a bedrock-

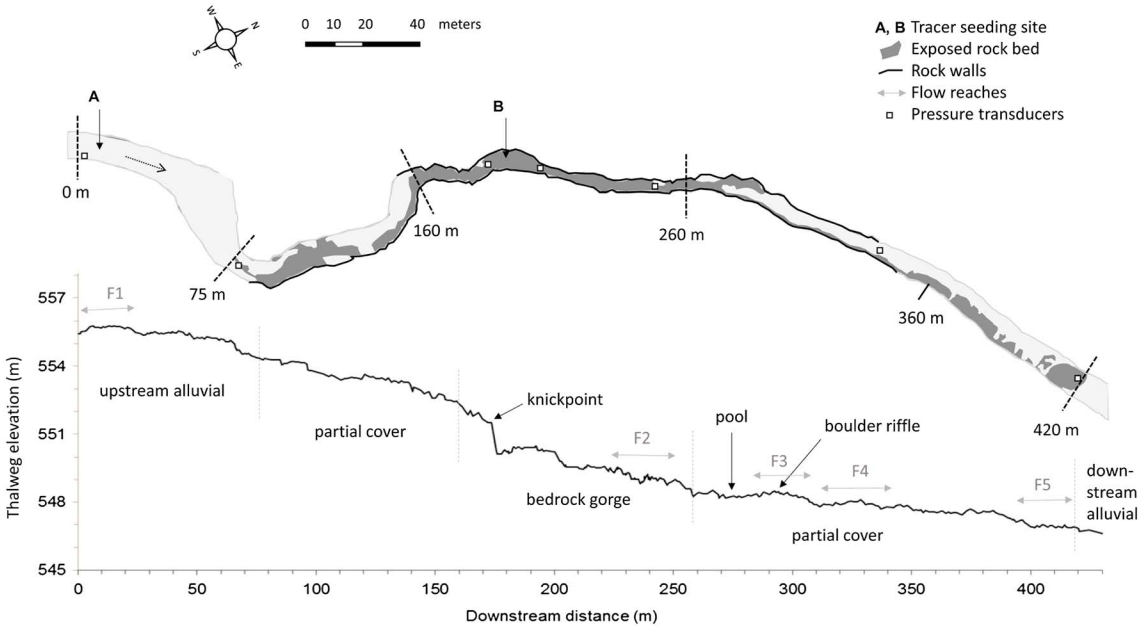

Figure 1. Map of study reach and longitudinal profile of thalweg. Map shows extent of rock walls, areas of exposed bedrock, and locations of flow measurement reaches (F1–F5) and stage loggers. Distances are downstream from first stage logger.

confined step-pool tributary followed similar scaling relations, but absolute travel distances were far lower in the tributary.

Here we report a controlled comparison of coarse bed load movement over contrasting bed types in the same stream. We tracked two sets of tracers for 19 months to investigate differences in mobility in an alluvial segment, over exposed bedrock, and in reaches with partial sediment cover on bedrock. We also calculated high-flow shear stresses in different parts of the channel to help interpret tracer dispersion. The results show clear differences in sediment mobility according to bed character and shear stress, and add to the limited database of direct field observations in bedrock channels.

2. Field Site

The experiment was carried out during 2013–2015 in Trout Beck, a small stream in the North Pennine hills of northern England (54°41.5′N, 2°23.3′W). The catchment is underlain by almost horizontally bedded limestone, shale, and sandstone [*Johnson and Dunham*, 1963]. Bedrock is covered in most places by thin glacial deposits and/or blanket peat. Small rapids or waterfalls, generally <1 m in height, have developed on resistant strata but are separated by longer alluvial reaches. The study site is a short rock gorge where the stream cuts through a thin (~4 m) band of massive limestone. Figure 1 shows the planform and longitudinal profile of the channel, and Figure 2 illustrates the changes in character along the stream. Downstream distances (x) in these and subsequent diagrams are measured from the first of seven pressure transducers which we installed along the reach in order to log water levels.

An unconfined upstream alluvial segment ($x < 75$ m; Figures 2a and 2b) is followed by a bedrock segment ($x = 75$–420 m), then another alluvial segment ($x > 420$ m). The bedrock segment has some exposed rock in its bed and banks everywhere but varies considerably in character. From $x = 75$ m the channel is confined on one side and has some exposed rock in its bed. Near-vertical limestone walls begin at 160 m, and at 175 m there is a small knickpoint with a 1.5 m drop into a plunge pool. This is followed by an almost straight and relatively narrow rock gorge. This has negligible sediment cover (Figures 2c and 2d) as far as 260 m but a partial cover, averaging about 60%, from 260 to 325 m (Figure 2e). The limestone walls of the gorge are blocky with sharp-cornered spurs and re-entrants. From 325 to 420 m the channel still has a bedrock floor with partial sediment cover (averaging about 40%), but its left bank is till or peat and the channel is wider (Figure 2f). The channel then reverts to fully alluvial.

Figure 2. Changes in channel character along the study reach: (a and b) upper alluvial segment and A-tracer seeding site, (c and d) rock gorge and B-tracer seeding site, (e) pool and boulder riffle near end of rock gorge, and (f) lower partial-cover channel. The arrows indicate flow direction; distances as in Figure 1.

Bed slope and channel width vary along the channel. The overall mean bed slope is 0.020, but the upstream and downstream alluvial channels are slightly flatter (0.015 and 0.016, respectively) and the sediment-free part of the gorge is slightly steeper (0.023). Bankfull channel widths also vary downstream: 10–15 m in the fully alluvial segments, 5–7 m in the rock-walled gorge, and 8–10 m in the partial-cover channel farther downstream. There are no tributaries, boulder steps, or woody debris.

The sediment cover consists mostly of gravel and cobbles, but boulders are present in places (e.g., Figure 2e). We know from previous fieldwork that an extreme flood in 2002, with an estimated return period of ~200 years, stripped all sediment from the gorge apart from these boulders. A partial sediment cover reformed within a year. Its extent and pattern have changed very little since then, and not at all over the duration of our tracer study. Most of the boulders are far coarser than any clasts in the upstream alluvial channel and may be former joint blocks detached by bed plucking or wall collapse during the gradual incision of the gorge. No bank collapse was observed during the study, so coarse sediment supply was entirely from upstream through fluvial transport during flood events. Bed load transport rates within the gorge therefore depended on the availability of sediment within the reach or supplied from upstream, together with the transport capacity and competence of the flow.

Annual precipitation in the catchment is ~2000 mm, mostly as frontal rainfall. Stage and discharge values at 15 min intervals have been logged since 1991 at an Environment Agency (EA) gauging structure 0.6 km downstream from the end of the study reach. A substantial tributary joins Trout Beck just upstream from the EA gauge, giving an increase in catchment area from 7.13 km^2 at the gorge to 11.46 km^2 at the gauging structure. The tributary has the same geology, superficial cover, and vegetation as the rest of the catchment and similar relief, so is assumed to be hydrologically similar. The mean flow and mean annual flood at the EA gauge are 0.62 $m^3 s^{-1}$ and 17.2 $m^3 s^{-1}$, and the highest flow during the study period was 14.2 $m^3 s^{-1}$. Scaling these numbers by the catchment area ratio (7.13/11.46 or 0.62) suggests values of about 0.4, 11, and 9 $m^3 s^{-1}$, respectively, at the study site. The flow regime is very flashy, with a lag of less than 3 h between rainfall and runoff peaks in well-defined events.

3. Experimental Design

Based on existing knowledge about bed load transport in steep alluvial channels, and standard assumptions in models of bedrock channel processes [e.g., *Lague*, 2010; *Johnson*, 2014; *Zhang et al*., 2015], we hypothesized that coarse-sediment transport capacity in different reaches of Trout Beck is a function of excess shear stress during high discharges. Excess shear stress may vary downstream if there are differences in total shear stress and/or the threshold stress varies according to bed character. Any such differences should be reflected in the mobility of tracer pebbles representative of the sizes available in the stream.

We denote excess shear stress by $\tau - \tau_c$ where $\tau = \rho g R S$ is the spatially averaged total fluid stress on the channel bed, τ_c is the critical or threshold stress for significant bed load transport, and R, S, ρ, and g denote, respectively, hydraulic radius, slope, water density, and gravity acceleration. The total shear stress for a given water discharge (Q) is higher in steeper and/or narrower channels, which in our study site means the rock-walled gorge. Threshold shear stress in alluvial channels is normally estimated by using Shields' criterion: $\tau_c/(\rho_s - \rho)gD = \tau^*_c \approx$ constant, where ρ_s denotes sediment density and D is a representative grain diameter of the bed material. Rock beds may have higher or lower τ_c than adjacent alluvial beds, depending on the topographic roughness of the rock surface at length scales consistent with grain diameters [*Hodge et al*., 2011; *Johnson*, 2014]. Where a stream crosses steeply dipping strata the increased bed roughness might result in a high threshold stress. However, in Trout Beck the stream flows along the dip and the exposed limestone in the floor of the gorge is notably smooth apart from small scallops and downstream-facing steps. We therefore expect τ_c to be lowest on exposed bedrock, and elsewhere to depend on the coarseness of the sediment cover.

These considerations led us to investigate the mobility of two sets of tracer pebbles, introduced at the same time and subsequently experiencing the same sequence of floods. We installed one set (A hereafter) at $x = 6$ m in the fully alluvial channel above the bedrock gorge and the other set (B hereafter) on exposed bedrock at $x = 195$ m near the head of the gorge. Our general hypothesis suggested three testable predictions about the mobility of the A and B tracers: (1) The B tracers would initially be more mobile than the A tracers, because of higher τ and lower τ_c. (2) Once the B tracers moved onto the partial sediment cover their mobility would decrease as τ_c increased, more so where the cover is coarser. Finally, (3) if/when the A tracers reached exposed bedrock above the knickpoint, their mobility would increase and they would start to behave more like the B tracers did initially.

4. Methods

4.1. Channel Characteristics

The topography of the channel sides and those parts of the bed exposed at low flow was surveyed by terrestrial laser scanning rectified by using control points mapped by differential Global Positioning System (dGPS). We also used dGPS to survey the thalweg longitudinal profile, 50 channel cross sections, the boundaries between exposed bedrock and sediment cover, and the footprints and protrusion of individual boulders with a maximum visible axis length exceeding 256 mm.

Grain size distributions (GSDs) of the sediment cover were obtained by 100-pebble counts in 14 small areas (typically ~10 m^2) spaced along the channel, to guide the design of the tracer experiment and help interpret its results. The bed GSDs vary greatly from place to place along the channel (Figure 3), with median diameters

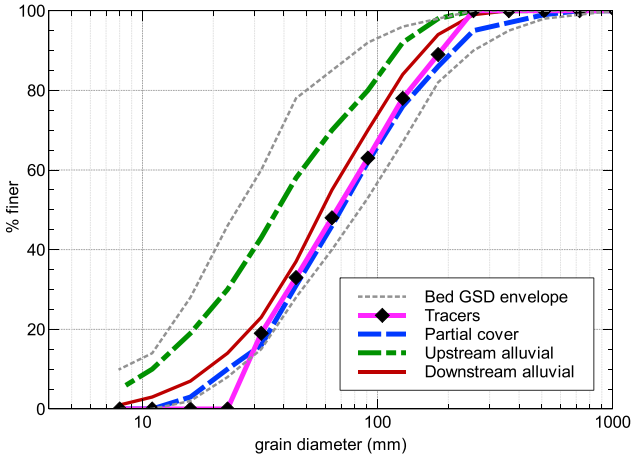

Figure 3. Bed and tracer grain size distributions. Envelope of 14 local bed grain size distributions is shown by broken grey lines. Averages for the upstream alluvial channel, the partial cover in the bedrock gorge, and the downstream alluvial channel are shown for comparison with the tracer size distribution.

(D_{50}) ranging from 27 mm to 84 mm. The coarsest GSDs are all from the partial sediment cover in the downstream part of the bedrock gorge. Averaging them gives a GSD with $D_{50} = 70$ mm and $D_{84} = 169$ mm for this part of the channel. The upstream alluvial channel has a finer bed: the average of the GSDs from it gives $D_{50} = 38$ mm and $D_{84} = 102$ mm, and the partial sediment cover where the stream approaches the knickpoint is similar. The bed at the start of the downstream alluvial channel is finer than the partial cover in the gorge; it has $D_{50} = 58$ mm and $D_{84} = 128$ mm.

4.2. Bed Load Tracers

Each set of tracers comprised 270 clasts obtained from the bed of the stream and spanning seven half-phi sieve size classes from 23 mm to 256 mm. Tracers finer than 23 mm could not be prepared because they usually split when drilled, and clasts larger than 256 mm were thought unlikely to move. The 181–256 mm tracers were measured, painted, and numbered in situ. All others were removed to the laboratory where their *a*/*b*/*c* axis lengths were measured and magnets were inserted in drilled holes. They were then painted, numbered, and returned to the field site. The tracers varied greatly in shape, with Corey sphericity values ($c/\sqrt{ab}$) from 0.11 to 0.89 (mean 0.51).

We decided to use the same GSD for both sets of tracers to allow direct comparison of the dispersion of a wide range of sizes over contrasting beds. The tracer GSD is superimposed on the bed GSDs in Figure 3. It is an approximation of the GSD of the partial cover in the downstream part of the gorge along which the B tracers were expected to travel, but with the 23–32 mm size class over-represented to compensate for the absence of $<$23 mm tracers. The tracer size range covers 88% of the range of sediment sizes in the gorge, omitting just 7% in the fine tail and 5% in the coarse tail, and the tracer D_{50} and D_{84} values of 75 mm and 165 mm are close to those of the bed. A consequence of using the same GSD for both sets is that the A tracers were coarser on average than the bed on which they were installed, which has 30% of $<$23 mm sediment and only 7% $>$128 mm (Figure 3). To allow for this when investigating threshold conditions for movement, we make two alternative analyses of A-tracer displacement, one based on all recovered tracers and the other excluding tracers coarser than 128 mm.

The A tracers were spread out as a loose 5×3 m patch on the surface of the upstream alluvial channel (Figure 2b), and the B tracers were spread out over a 4×3 m area of exposed bedrock in the gorge (Figure 2c). Tracers placed loosely on a gravel bed tend to be unrepresentatively mobile until they become worked into the active layer, so we expected the results of the first A-tracer survey to be anomalous. The outcome is discussed below (section 5.1). We surveyed tracer dispersion on six occasions in the first 9 months, with a final search 19 months after installation. Tracers were located by using magnetometers with a detection range of $>$0.5 m. Only 2–9% of tracers found in sediment-covered areas were not visible in the surface layer, and none of them was buried by more than ~0.1 m, so disturbance by searching was minimal. Recovered tracers were identified, mapped by dGPS and replaced where found.

Travel distances reported below are mostly straight-line distances, either between locations in successive surveys or from the original installation site. The upper alluvial channel in which the A tracers were installed is fairly straight, and so is the gorge downstream from where the B tracers were installed, so any underestimation of actual travel distances in these parts of the channel is small and does not compromise analyses of relative mobility or size and shape selectivity. The channel immediately above and below

the knickpoint is more sinuous (Figure 1) so A-tracer travel distances through this part were calculated as a series of straight segments.

4.3. Discharge and Stage

The cumulative and peak discharges between surveys, and bulk hydraulic conditions in different parts of the study reach at various discharges, were estimated from measurements within the reach together with EA discharge data from 0.6 km downstream. Water levels were logged by using pressure transducers at seven locations along the reach (Figure 1). Sixty discharge measurements by sudden-injection salt dilution or current meter were made in conditions ranging from base flow to minor flood (0.1–2.1 $m^3 s^{-1}$) and gave a well-defined stage rating curve. We could not make measurements at higher discharges because of safety considerations and the flashiness of the stream. A linear regression of measured discharge in the study reach against the EA discharge at the same time has a slope of 0.65 with a 95% confidence interval of ±0.02. This is very close to the catchment area ratio of 0.62 (section 2), and we reasoned that the same should be true on average for flows higher than 2.1 $m^3 s^{-1}$ during floods caused by frontal rainfall rather than localized convective storms. The peak discharges and cumulative discharges considered in later sections are scaled from the EA record by using a conversion factor of 0.65.

This scaling was also used to create stage-discharge rating curves for each pressure transducer. To do this, we selected six large frontal-rainfall floods and noted the times when different high discharge values were passed on the rising and falling limbs of the EA hydrograph. We then multiplied these discharges by 0.65 and matched them to the immediately previous logged stage (h) at each pressure transducer. These high-flow h, Q pairs were added to the lower flow pairs obtained by using salt dilution, and curves of the form $Q = a(h - h_0)^b$ were fitted by using least squares. Here h_0 is an offset that varies according to the position of the transducer within the cross section.

4.4. Bed Shear Stress

Detailed measurements of channel geometry and water level in five short (24–28 m) reaches, labeled F1–F5 in Figure 1 and hereafter, were used as explained below to calculate how shear stress varies with discharge in those reaches. Less reliable estimates were also made by using the same methods for four intervening stretches. These nine sets of estimates cover most of the channel length that the tracers traversed.

Reaches F1–F5 were chosen for their contrasting bed character and relevance to tracer dispersion. F1 is in the upstream alluvial channel where the A tracers were installed and F2 is in the exposed bedrock gorge just past where the B tracers were installed. F3–F5 all have a partial sediment cover but of differing extent and caliber. In each reach we surveyed 7–10 cross sections, and also the water surface profile at a measured discharge of ~1 $m^3 s^{-1}$ using closely spaced dGPS measurements. This allowed calculation of the overall water surface slope (S_w) and the wetted perimeter (P), cross section area (A), and mean velocity (v) at each cross section at that discharge. Values of these variables at a set of higher discharges were then calculated by raising the water surface elevation at each cross section in accordance with the stage rating curves for the pressure transducers immediately upstream and downstream from the reach concerned, with contributions weighted inversely by distance. This procedure allows for any change in water surface slope with stage. It enabled calculation of reach-average hydraulic radius R as $<A>/<P>$, where angle brackets denote averages over the cross sections within the reach. Finally, the mean shear stress was calculated as $\tau = \rho g R S_e$, where S_e is the energy slope obtained by adjusting S_w for any difference in velocity head between the cross sections at either end of the reach.

There are three sources of uncertainty in these calculations of shear stress: scatter of stage readings around the rating curves (residual standard deviation 0.02–0.05 m), precision of dGPS elevation measurements (±0.02 m), and downstream variability in channel slope and cross-section geometry. The first two affect the accuracy of S_w, and the third affects the accuracy of R. We calculate that S_w is accurate to within ±0.002 in F2 and ±0.001 elsewhere, giving an uncertainty of 3–7% in the estimated reach slope. The standard error of reach-average R in F1–F5 at high discharges is 0.01–0.03 m or 2–7%. Combining these uncertainties suggests a potential error of 4–10% in absolute values of shear stress in F1–F5. This is small compared to the between-reach differences in shear stress at a given discharge (section 5.2).

Mean shear stresses in another four parts of the channel were obtained in essentially the same way but using information from only two or three surveyed cross sections. Estimates were made for the 35 m of alluvial

Table 1. Cumulative Movement of Tracers Installed on Alluvial (A) and Bare Rock (B) Beds

Survey Number and Date (dd/mm/yy)	Recovery Rate (%)		Mean Travel Distance (m) and Standard Error		Median Travel Distance (m)		Maximum Travel Distance (m)	
	A	B	A	B	A	B	A	B
0 (29/8/13)				Tracers installed				
1 (9/10/13)	100[a]	58	0[a]	51 ± 2	0	65	15	113
2 (4/11/13)	91	68	2.4 ± 0.2	70 ± 2	2	75	18	134
3 (11/12/13)	89	74	3.4 ± 0.2	73 ± 2	2	75	21	140
4 (19/1/14)	84	53	9 ± 1	94 ± 4	6	84	34	234
5 (30/3/14)	83	72	18 ± 2	99 ± 3	14	90	66	234
6 (26/5/14)	84	69	17 ± 2	107 ± 4	13	93	54	302
7 (9/4/15)	66	48	37 ± 5	151 ± 6	23	118	420	341

[a]Only 10 of 270 installed tracers had moved >1 m and were surveyed. All others are assumed not to have moved.

channel immediately downstream from F1, using its final cross section and two others; the 30 m of rock gorge extending upstream from F2 to the nearest pressure transducer; the 30 m long rock pool area between the sections at the downstream end of F2 and the upstream end of F3; and the 51 m of partial cover between F4 and F5. In each case the water surface slope at different discharges is known to the same accuracy as in F1–F5. The mean hydraulic radius is less reliable, being based on only 2–3 widely spaced cross sections instead of 7–10 closely spaced sections. However, omitting all but the first and last sections in F1–F5 alters the reach-average R for those reaches by only 1–9%. This suggests that the estimates of shear stress in the four additional reaches can be used to indicate relative differences in shear stress, even if the absolute values are imprecise.

4.5. Relative Transport Capacity

The shear stress estimates for F1–F5 were used to make indicative calculations of how bed load transport capacity differs between the upstream alluvial channel (represented by F1), the exposed rock in the gorge (F2), and the partial-cover reaches farther downstream (F3–F5). This was done in the way proposed by *Johnson* [2014], using the *Meyer-Peter and Müller* [1948] transport equation with different values of threshold Shields stress (τ^*_c) for sediment cover and exposed bedrock, and neglecting wall effects. The overall transport capacity of a reach is then calculated as an area-weighted average of the bedrock and sediment-cover transport capacities per unit width. As in *Johnson* [2014], the threshold Shields stress for exposed bedrock was calculated by substituting the ratio D_s/D_r into the hiding function of *Wilcock and Crowe* [2003]. Here D_s is the representative bed load grain size used in the transport equation (38 mm, the D_{50} of the alluvial bed which supplies sediment to the rock gorge) and D_r is a roughness length scale for exposed rock, expressed as a grain diameter. We made calculations by using various combinations of τ^*_c in the range of 0.03–0.08 for the sediment cover and $D_r = 10$ to 30 mm for rock roughness. The corresponding values of τ^*_c for exposed bedrock ranged from 0.018 to 0.068 but were always lower than for the sediment cover. The qualitative pattern of differences in transport capacity between reaches was the same for most combinations of the two parameters.

5. Results

Summary statistics of the dispersion of the two sets of tracers are presented in section 5.1, which also describes how movement between successive surveys relates to peak discharge and cumulative discharge above a threshold. Section 5.2 summarizes the results of calculations of shear stress in different parts of the channel and the implications of those calculations for relative transport capacity. Section 5.3 describes how the spatial pattern of tracer dispersion evolved over time and how it relates to the spatial patterns of shear stress and sediment cover. The size and shape selectivity of tracer dispersion is analyzed in section 5.4.

5.1. Tracer Dispersion in Relation to Flood Events

Both sets of tracers dispersed gradually downstream, as illustrated in Table 1 by summary statistics of cumulative movement since installation. Recovery rates were generally high in the first 9 months (surveys 1–6: 83–91% for set A and 53–74% for set B) but lower in the final survey 10 months later. Some of the lost

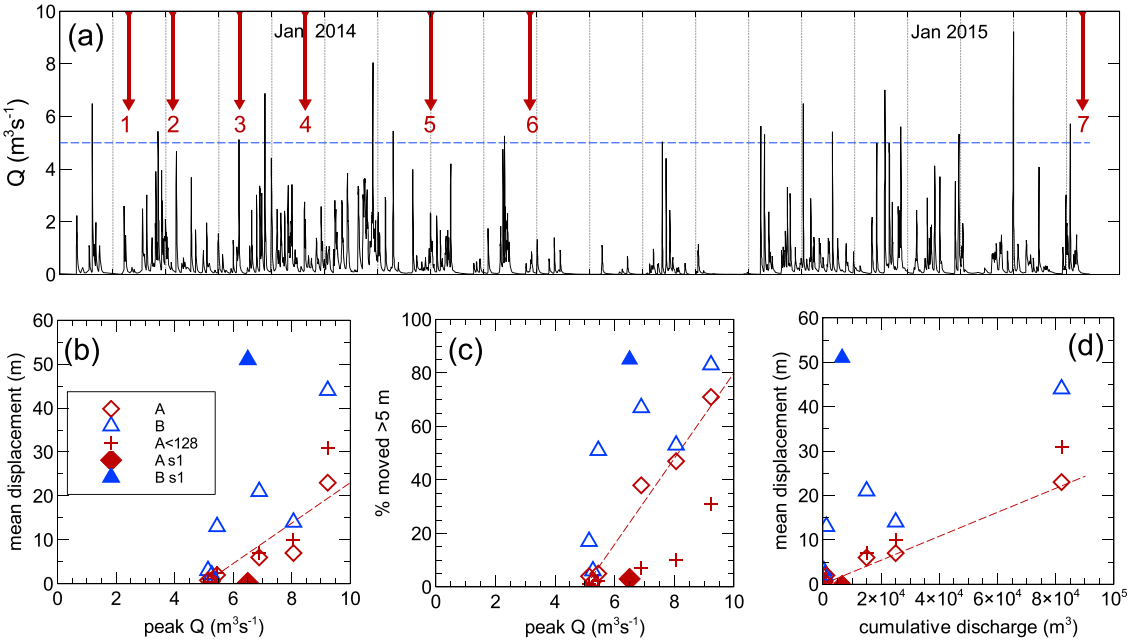

Figure 4. (a) Timing of surveys with respect to hydrograph. (b) Mean intersurvey displacement of A and B tracers during intervals with different peak discharges. Displacement from installation to first survey (s1 in key) is shown by solid symbols. Displacement of A tracers finer than 128 mm is shown by crosses. (c) Percentages of A and B tracers moving >5 m during intervals with different peak discharges. (d) Mean intersurvey travel distances in relation to cumulative discharge volume above a threshold of 5 $m^3 s^{-1}$. Linear trends shown in Figures 4b–4d are visual fits to the A tracers.

tracers, particularly from set B which was installed farther downstream, may have traveled beyond the search area, but nearly all tracers missed during one of the first four surveys were found in a subsequent survey. The grain size distributions of set B tracers not recovered in the last two surveys were almost the same as the size distribution of those that were found, but in set A there was a tendency for the lost tracers to be smaller than average.

The cumulative average distances show that the A tracers dispersed more slowly than the B tracers. We examine in detail later (section 5.3) how this difference relates to spatial differences in bed type and shear stress. Here we focus on differences over time, by considering tracer mobility during the intervals between successive surveys and comparing it with the irregular incidence and variable magnitude of flood events (Figure 4a). Floods during the study period were of moderate magnitude when compared with the long-term record from the EA gauge and never exceeded the mean annual flood.

Figures 4b and 4c compare tracer mobility between successive surveys with the peak discharge during the intervening period. Mobility is quantified in two ways: mean intersurvey displacement and percentage of tracers that moved more than 5 m. The sample size is the number of tracers recovered on both occasions and ranges from 109 to 187 for set A (40–69% of installed tracers) and 100–169 for set B (37–63%). Both plots show that mobility tends to increase with peak discharge. The A tracers were most mobile during the long interval between surveys 6 and 7, which included the event with the highest peak discharge of the study period and nine other floods with peaks above 5 $m^3 s^{-1}$ (Figure 4a). The B tracers were more mobile in this interval than in any other apart from the first one after installation, when they were dispersing over exposed bedrock.

The A tracers, in contrast, were least mobile during the first interval. In survey 1 almost all of them were still in their original patch (Figure 2a). To avoid disturbing them we only mapped the 10 tracers that had moved out of the patch, so the statistics for this survey in Table 1 and Figure 4 are based on the assumption of 100% recovery with 260 tracers not moving. As noted above (section 4.2) we had expected that these loosely placed tracers would disperse rapidly. A possible explanation for why this did not happen is that, as noted in section 4.2, the tracer GSD included a higher proportion of 128–256 mm cobbles than is present in the bed at the installation site. These coarse tracers may initially have sheltered the small- and medium-sized tracers

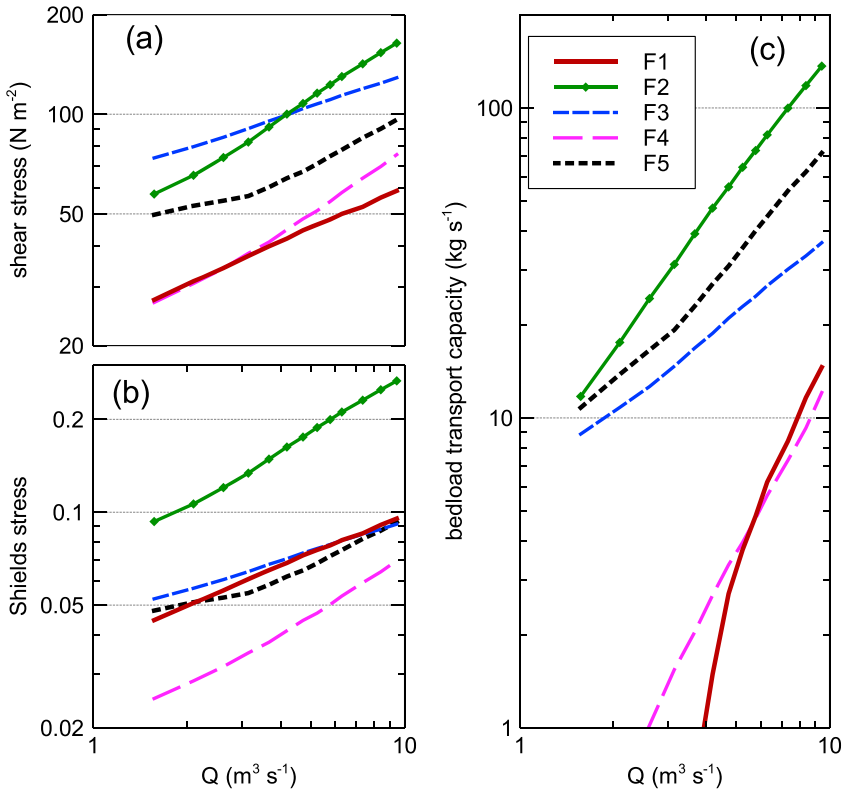

Figure 5. Variation of (a) mean bed shear stress, (b) Shields stress, and (c) bed load transport capacity with water discharge in reaches F1–F5 of the study site (see Figure 1 for locations).

that were expected to move readily from their loose initial positions. However, any such effect was temporary because by survey 2 all tracers, whether coarse or fine, had moved out of the initial patch and become integrated into the bed surface. The mobility of the A tracers is slightly higher if the 128–256 mm size classes are excluded (Figures 4b and 4c), but it remains less than the mobility of the B tracers, and the correlation with peak discharge is still present.

Neither set of tracers moved significantly between surveys 2 and 3 (maximum discharge 5.1 m^3 s^{-1}) or between surveys 5 and 6 (maximum discharge 5.3 m^3 s^{-1}), and the trends in Figures 4b and 4c are consistent with a threshold discharge of about 5 m^3 s^{-1}. This is the threshold for >23 mm clasts; the threshold for fine gravel will be lower. Since mobility should depend on the duration of flows above threshold as well as the peak discharge we also plot mean intersurvey displacement against cumulative discharge above a notional threshold of 5 m^3 s^{-1} (Figure 4d). The initial movement of both sets of tracers remains anomalous as already discussed (A abnormally inactive, B abnormally mobile), but their subsequent mobility now follows an approximately linear trend with less scatter than when using peak discharge.

5.2. Shear Stress and Relative Transport Capacity

Our calculations of mean bed shear stress in reaches F1–F5 show that it varies considerably along the channel (Figure 5a). At any given discharge it is highest in F2 (exposed bedrock gorge) and F3, and lowest in F1 (upstream alluvial channel) and F4, with F5 intermediate. However, as noted in section 4.1, there are also considerable differences in the caliber of the sediment cover in the different reaches. When the absolute values of shear stress in each reach are converted to Shields stresses by using the local bed D_{50}, the downstream pattern changes: reaches F1, F3, and F5 have almost identical Shields stresses at any given discharge, and F4 has the lowest values (Figure 5b). Reach F2 contains no sediment so is scaled by using the D_{50} (38 mm) of the upstream alluvial channel that supplies sediment to the gorge. It has by far the highest Shields stress of all at any given discharge.

Rating curves of estimated transport capacity as a function of discharge are shown in Figure 5c. The curves shown are for a rock roughness (D_r) of 10 mm and a threshold Shields stress (τ^*_c) of 0.06 for sediment cover. Calculations for all combinations of D_r in the range of 10–30 mm and τ^*_c in the range of 0.03–0.08 show the same qualitative pattern of results: transport capacity is highest in the sediment-free bedrock reach F2, also high in F5 (80% exposed bedrock), intermediate in F3 (30% bedrock), and lowest in F1 (upstream alluvial reach) and F4 (30% bedrock). The calculations for the partial-cover reaches F3–F5 depend heavily on the untested, but plausible, assumption that the bare-rock and sediment-cover transport capacities per unit width can be weighted in proportion to area as measured at low flow. However, even if all bed load in those reaches was assumed to move over exposed rock rather than sediment, for example, because cover temporarily disappeared or entrainment was preferentially from its edges, these reaches still would not have such a high transport capacity as the sediment-free bedrock gorge (F2). Likewise, the order-of-magnitude difference between the calculated transport capacities of F2 and F1 far exceeds the uncertainty associated with the precise values of τ^*_c for sediment and exposed rock.

The shear stress calculations for other parts of the channel are less reliable but help complete the picture of spatial variation. The shear stress immediately downstream from F1 is slightly higher than in F1 and increases slightly more rapidly with discharge. The shear stress immediately upstream from F2 is lower than in F2 but much higher than in F1 at all discharges. The boulder-strewn bedrock pool between F2 and F3 has a lower shear stress than either of those reaches at all discharges. The partial-cover reach between F4 and F5 has a higher shear stress than in F4 but lower than in F5; however, the differences reduce as discharge increases, as can be seen from the convergence of the F4 and F5 curves in Figures 5a and 5b. The downstream variation in shear stress revealed by these reach-by-reach calculations is one of the factors we consider when discussing the spatial pattern of tracer dispersion in the next section.

5.3. Spatial Pattern of Tracer Dispersion

In flume-like conditions of regular channel geometry, a homogeneous bed, and uniform flow the mobility of tracer clasts should be the same everywhere. In Trout Beck, however, there are big changes along the channel in the extent and caliber of sediment cover, in shear stress, and by implication also in transport capacity. Here we investigate how these along-channel changes are reflected in irregularities in the pattern of tracer dispersion. We do this by inspecting the cumulative distribution curves of tracer recovery position in successive surveys and by comparing intersurvey travel distances in different parts of the channel.

The cumulative distribution curves of where the A and B tracers were found in successive surveys are shown in Figure 6. The distributions for surveys 3 and 5 are omitted since they are near-duplicates of those for surveys 2 and 6, respectively. To aid interpretation, Figure 6 also shows the patterns of downstream variation in shear stress and sediment cover. Shear stress estimates are shown for 5 and 10 $m^3 s^{-1}$, the approximate range of competent discharge during the study period. Figure 6c shows the percentage cover in successive 10 m lengths of the channels, as determined from the surveyed boundaries between exposed bedrock and sediment cover. It also shows the number of boulders per 10 m. The greatest concentration of boulders is in the 70% sediment cover in flow reach F3 at $x = 285$–305 m. This reach is steeper (see Figure 1) and hydraulically much rougher than the exposed bedrock immediately upstream from it, so in all but the highest discharges it has much the same backwater effect as riffles do in gravel bed rivers. We call it the "boulder riffle" hereafter and use "pool" for the mainly rock-floored backwater zone at $x = 260$–285 m, which experiences lower shear stresses than in F2 immediately upstream and F3 immediately downstream (Figure 6a). The largest boulder of all, 1.15 m in diameter, is in this pool at $x = 263$ m.

The tracer distribution curves for surveys 1 and 2 in Figure 6b illustrate in detail the huge initial difference in mobility between the A and B tracers. Only 10 of the A tracers had moved out of the initial patch by survey 1, and 86% of the 270 installed tracers were recovered within 5 m of their initial position in survey 2. In contrast, only 26% of the B tracers were found less than 60 m from their initial position in survey 1, and we do not think we missed any in this sediment-free part of the channel. The initial patch of B tracers was intact at a discharge of 1 $m^3 s^{-1}$ a week after installation, but dispersed almost completely during a 6.5 $m^3 s^{-1}$ flood shortly before survey 1. By survey 2, after a second event peaking at 5.4 $m^3 s^{-1}$, only 14% of the B tracers had traveled less than 60 m from their starting position. In these early surveys the majority of recovered B tracers were found in the pool immediately upstream from the boulder riffle, as shown by the steepness of the cumulative curves at $x = 260$–285 m in Figure 6b. In survey 1 only one B

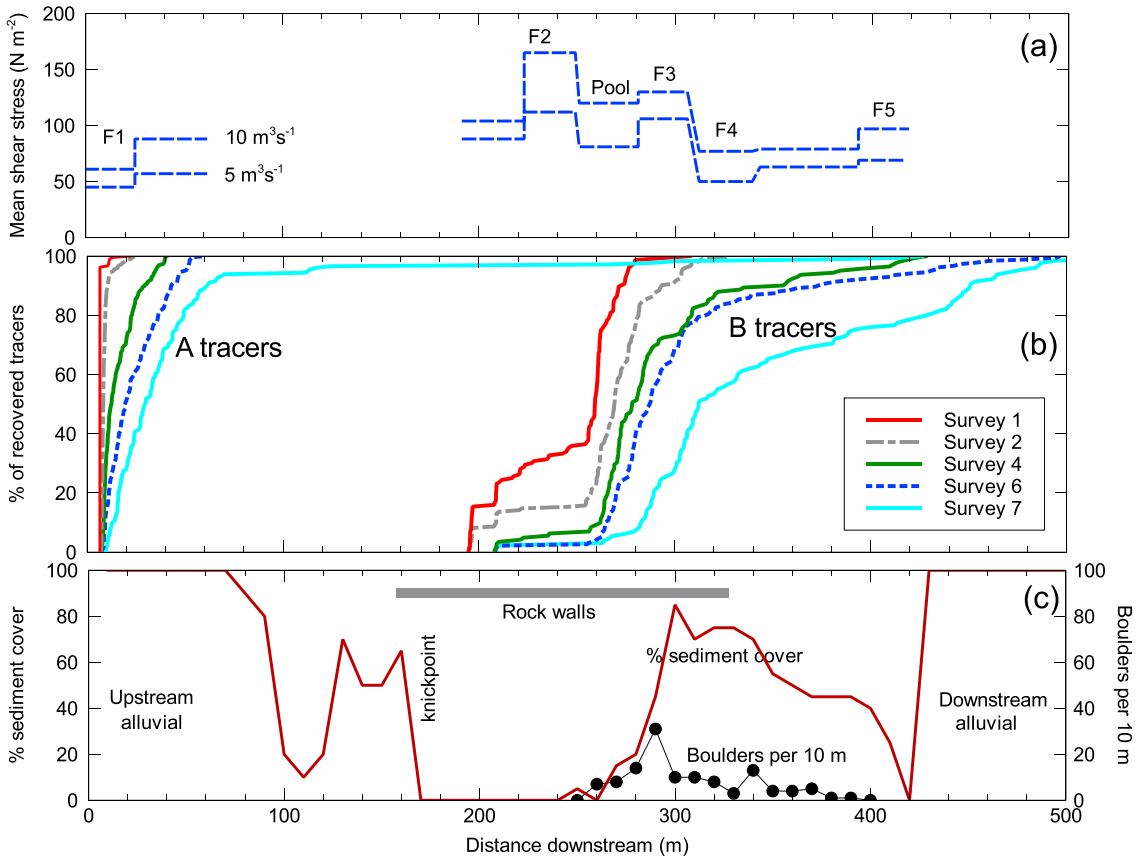

Figure 6. Spatial patterns of (a) shear stress at competent discharges, (b) tracer dispersion in successive surveys, and (c) percentage sediment cover and boulder density.

tracer was found in the boulder riffle itself and none farther downstream, but by survey 2, 11% of recovered tracers were in the boulder riffle and 4% farther downstream.

This contrast between the initial dispersion of the two sets of tracers is consistent with the differences in shear stress between the reaches in which they were installed or into which they moved (Figure 6a). The A tracers experienced much lower shear stresses than the B tracers in the first flood, and the difference in excess shear stress is even greater if the assumption of a lower threshold stress on bare rock is correct. The accumulation of B tracers in the pool is consistent with the downstream decrease in shear stress from the rock gorge (reach F2 in Figures 5 and 6a) to the pool, whose lower bed gradient is accentuated by the backwater effect of the boulder riffle immediately downstream from it. Shear stress in the boulder riffle itself (F3 in Figures 5 and 6a) is higher than in the pool but slightly lower than in F2. Moreover, the extent and coarseness of its sediment cover implies a higher threshold stress than farther upstream, and thus a lower theoretical transport capacity (compare F3 with F2 in Figure 5b).

The tracer distribution curves for surveys 4 and 6 (Figure 6b) show that the A tracers continued to disperse slowly along the upper alluvial reach. They moved a mean distance of 7 m (standard error ±1 m) between surveys 2 and 4 (two competent floods, peak discharge 6.9 $m^3 s^{-1}$) and another 7 ± 1 m between surveys 4 and 6 (three competent floods, peak discharge 8.1 $m^3 s^{-1}$). The B tracers continued to be more mobile than the A tracers during these two periods. The few that were still on exposed rock within 60 m of their starting position moved an average of 47 ± 7 m between surveys 2 and 4 and 30 ± 9 m between surveys 4 and 6. The many B tracers that were already into the pool or boulder riffle were less mobile than that but more mobile than the A tracers, with mean displacements of 19 ± 3 m between surveys 2 and 4 and 9 ± 1 m between surveys 4 and 6. This continued dispersion meant that progressively fewer B tracers were found in the pool, and more in the boulder riffle or farther downstream. The elongated upper tail of the B-tracer distribution in surveys 4 and 6

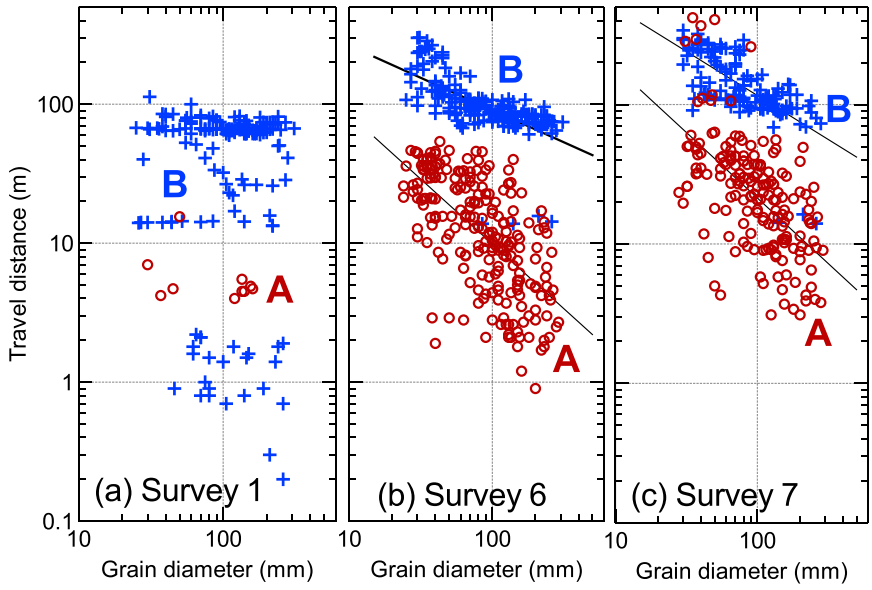

Figure 7. Tracer travel distances in relation to grain size, with power law fits where the exponent is significantly different from zero ($p < 0.05$). Distances are cumulative from installation. The A tracers first encountered rock at 69 m, and the B tracers first encountered sediment at 65 m.

suggests that once tracers progressed past the pool and boulder riffle they became more mobile despite the relatively low shear stresses in this part of the channel ($x > 305$ m onward in Figure 6; F4 in Figure 5). The mean displacement between surveys 4 and 6 of 26 tracers that were already past the boulder riffle was 30 ± 6 m, compared to 9 ± 1 m for tracers starting in the pool or boulder riffle at the same time. However, the detailed data show that these frontrunners were all finer than 64 mm and might thus be intrinsically more mobile than the tracer population as a whole.

The A tracers as a whole continued to be less mobile than the B tracers during the long and flood-rich interval between surveys 6 and 7 (mean A-tracer displacement 23 ± 4 m, compared to 44 ± 5 m for the B tracers), but at some time during this period the frontrunners of set A reached the exposed rock that begins 69 m from their starting position. Five were recovered upstream from the knickpoint, one in the pool, two in the boulder riffle, two on partial cover farther downstream, and one at the start of the lower alluvial reach. These 11 tracers had traveled 68–380 m since survey 6, making them more mobile than the B tracers in this period. In contrast, the mean and maximum displacements of the A tracers that remained in the upper alluvial channel in this final period were only 6 m and 12 m.

5.4. Size and Shape Selectivity

The analysis so far has considered the dispersion of the two sets of tracers in a collective way, without regard to the size or shape of individual tracers. Since, the sets have the same grain size distribution and the same range of shapes any tendency for selective transport does not bias the comparison between A and B tracers, but the selectivity (or not) of transport is of interest in itself. We investigated it by multiple regression analysis of the travel distances of individual tracers from installation up to a particular survey (L, in meter) in relation to grain size (b axis diameter in mm, D) and shape (Corey sphericity index, C). The variables were log-transformed to make the trends more nearly linear and the scatter more nearly homoscedastic. We analyzed the distances traveled by all tracers recovered in surveys 1, 6, and 7, with the exception of the A tracers in survey 1 where only the 10 tracers that had left the initial patch were considered.

The initial dispersion of both sets of tracers was unselective (Figure 7a). The multiple regression of log L on log D and log C for the 10 A tracers has an R^2 value of only 0.16 with neither predictor significant at even the 0.10 level. The B tracers had dispersed much more, with the exception of 24 that were still within 10 m of their starting position and form a separate cluster of data points in Figure 7a. Regressions for these 24 tracers,

for the other 132 recovered B tracers, and for the combined total of 156 all have very low R^2 values (0.01–0.12) with neither predictor significant at the 0.10 level.

In contrast, the data from surveys 6 and 7 (Figures 7b and 7c) show a clear tendency for smaller tracers to have traveled farther, whether they started in the upper alluvial channel (A tracers) or on exposed bedrock (B tracers). There is considerable scatter, as expected because of the strong stochastic element in grain entrainment and step length, but the regression analysis shows that the effect of D on L is highly significant ($p < 0.001$) in all four cases. There is also a significant ($p < 0.05$) shape effect in the case of the A tracers, with more spherical tracers tending to travel farther after controlling for the effect of grain size. It is, however, very much a secondary effect: log C alone explains only 12% (survey 6) and 2% (survey 7) of the variance in log L, whereas log D alone explains 40% and 34%. Shape has no significant effect on B-tracer travel distances, but log D explains 43–46% of the variance in log L.

These analyses show that the initial dispersion of the B tracers over exposed rock was unselective, but their later transport in a channel with more sediment cover than bare rock was size selective, with smaller tracers tending to travel farther. The dispersion of the A tracers, which was entirely over sediment except for the frontrunners in survey 7, was size selective once the initial artificially placed patch had dispersed. It was also shape selective to a small but statistically significant extent, with more spherical tracers tending to travel farther than others of similar size.

6. Discussion

The observed pattern of dispersion of the two sets of tracers in Trout Beck (Table 1 and Figure 6) was consistent with all three of the predictions made in section 3. The B tracers dispersed much more rapidly at first, over bare rock, than the A tracers did in the upstream alluvial channel. Once the B tracers approached and entered the part of the gorge with a mainly sediment-covered bed they dispersed less rapidly, particularly in the part with many boulders. And although the A tracers dispersed slowly during most of the experiment, their frontrunners traveled long distances once they reached exposed rock late on in the experiment.

This may be the first direct demonstration of a difference in transport capacity between a reach with exposed bedrock and the alluvial channel immediately upstream. The comparison between the two sets of tracers is a controlled field experiment insofar as the A tracers, installed in the upstream alluvial channel, had the same grain size distribution as the B tracers installed on bare rock and the two sets experienced the same sequence of floods. The dispersion of the A tracers was consistently slower than that of the B tracers, with the exception of the 11 frontrunners of set A that reached bare rock after survey 6 and sped up.

The observed difference in behavior can be understood in terms of particle dynamics. Pebbles on a smooth rock floor can be entrained easily because of low friction angles and high near-bed velocity, and once moving they have a low probability of stopping before they reach a sediment patch. Transport steps are therefore relatively frequent and long. This perspective also helps explain the lack of size or shape selectivity in the initial dispersion of the B tracers, in contrast to the selective transport of both sets of tracers when entrained from a partial or complete sediment cover with a wide range of pocket geometry. Unselective transport was also observed by *Hodge et al*. [2011] in a bedrock channel with only 20% sediment cover and was explained in similar terms. One implication is that any bedrock channel model that includes a range of grain sizes should use a hiding function for transport over sediment, but not over smooth exposed rock.

The observations are also consistent with reach-scale rather than grain-scale considerations. The general hypothesis from which we derived our specific predictions in section 3 is that bed load transport capacity depends on excess shear stress. This is widely accepted for gravel bed rivers and is a basic assumption in several recent models of bedrock channel processes [e.g., *Lague*, 2010; *Johnson*, 2014; *Zhang et al*., 2015]. The Trout Beck results fit this framework and support its use in future work on bedrock channels. A key finding from our hydraulic calculations is that the Shields stress at any given discharge in the part of the gorge with no sediment cover is considerably greater than in the wider and less steep alluvial channel upstream from it (Figure 5b). This would give a substantial difference in transport capacity even if threshold stress was the same for smooth bare rock as for alluvium, and our calculations using a plausibly lower threshold stress for exposed rock indicate an order-of-magnitude difference between the transport capacities of the two reaches

(Figure 5c). Calculated Shields stresses for the partly sediment-covered lower part of the gorge, in which the B tracers were concentrated during most of the experiment, are lower than in the bare-rock gorge where rapid initial dispersion occurred. As demonstrated in section 5.3, all of this is in qualitative agreement with the observed differences in tracer mobility.

The pattern of dispersion was, however, more complicated than a simple difference between high mobility over bare rock and low mobility over sediment patches. The irregular variation in shear stress along the channel (Figure 6a) is one reason for this, but there are also downstream changes in the coarseness of the sediment cover (and thus in threshold shear stress) and in the extent of sediment cover (and thus the opportunity for tracers to disperse over rock rather than sediment). In view of this complexity we have not attempted to collapse tracer travel distances in different parts of the channel and at different times onto a single nondimensional scaling, such as the one proposed by *Phillips and Jerolmack* [2014]. Nor have we investigated scaling relations for virtual velocity in different parts of the channel [e.g., *Ferguson and Wathen*, 1998], since virtual velocity depends on threshold discharge and whether/how this varies locally along Trout Beck is poorly constrained. A consistent qualitative explanation for most of the observed behavior can nevertheless be provided by considering how the patterns of downstream variation in shear stress and bed character combine to create differences in excess shear stress and thus transport capacity. The main initial accumulation of B tracers in the pool, and subsequent concentration in the boulder riffle, can both be understood in these terms. The pool has very little sediment cover, and presumably the same low threshold stress as immediately upstream, but it has a much lower energy slope and consequently a lower shear stress (Figure 6a) and excess shear stress. The boulder riffle experiences higher shear stresses than in the pool, but slightly lower than where the B tracers were installed, and its extensive coarse sediment cover has a relatively high threshold stress with a consequent reduction in transport capacity.

The boulder riffle had a significant effect on tracer dispersion because, although short, it acted as a bottleneck impeding the movement of the B tracers. It did this both through the propensity of its coarse sediment cover to trap moving grains and through its backwater effect on flow and transport capacity in the pool immediately upstream. However, Figure 5c suggests that it does not restrict the throughput of sediment supplied naturally from the upstream alluvial channel (F1). Instead, F4 rather than F3 is the bottleneck for this natural sediment supply for some combinations of the parameters affecting the curves in Figure 5c. With other combinations, all sediment supplied by F1 can be transported right through F2–F5 to the lower alluvial channel. These calculations are sensitive to the assumed threshold shear stress for the sediment cover in each reach. We calculated the threshold stress from the D_{50} grain size of the cover, but this probably underestimates the effective threshold in reaches containing immobile boulders which exert form drag on the flow [*Yager et al*., 2007]. If so, the underestimation will be most severe in F3 which has the highest concentration of boulders (Figure 6c). The transport capacity of this reach (and to a lesser extent that of F4) might therefore be considerably lower than is shown in Figure 5c. This could explain why these boulder-rich parts of the channel are where sediment cover started to re-form after being stripped in the 2002 flood mentioned in section 2. The sediment-trapping effect of boulders has also been observed in flume experiments with sediment supply well below capacity [*Chatanantavet and Parker*, 2008]. This leads us to speculate about the possible long-term role of boulders in inhibiting channel incision into bedrock. If the lithology is such that boulder-sized blocks are released into the channel, either by bed plucking or by wall collapse, they will tend to increase sediment cover and make it coarser. This might make incision self-limiting, as *Shobe et al*. [2016] and *Thaler and Covington* [2016] suggest could happen if the steepening of valley sides during incision releases coarse sediment that accumulates in the channel.

Our analysis of tracer dispersion between successive surveys suggested that mean travel distances increased approximately linearly with the volume of runoff above a threshold of 5 $m^3 s^{-1}$ (Figure 4d). A similar linear relation was found by *Olinde and Johnson* [2015] in a steep but predominantly alluvial channel. The existence of a threshold discharge is consistent with the presence of a threshold shear stress in standard rate laws for bed load transport [e.g., *Meyer-Peter and Müller*, 1948]. Many recent models of bedrock channel processes use a relation of this type to calculate transport capacity, but sediment supply is often approximated as a simple power function of water discharge with no threshold [e.g., *Lague*, 2010]. There is a conceptual inconsistency here if the supply is mainly or entirely from an upstream alluvial channel, which presumably should also follow an excess-stress transport law and thus supply no sediment below a threshold discharge. Our calculation for reach F1 of Trout Beck in Figure 5c shows this kind of relation, and a threshold of 5 $m^3 s^{-1}$ is exceeded less

than 1% of the time. However, while our 23–256 mm range of tracer grain sizes covers 88% of the size distribution of the partial sediment cover in the bedrock gorge, the upstream alluvial bed contains 30% of $<$23 mm sediment which presumably moves at lower discharges. The power law assumption for sediment supply may therefore be an acceptable approximation, as has been found for transport rates of all sediment $>$0.25 mm in gravel bed rivers with abundant fine sediment [*Barry et al*., 2004].

The precise pattern of downstream variation in shear stress, threshold stress, and sediment mobility in Trout Beck is site specific, but an increase in transport capacity relative to sediment supply must exist in other alluvial-to-bedrock transitions. Considering why and how this can occur helps put our findings into a wider context. Three possibilities are a downstream increase in shear stress because the channel becomes narrower where constricted by rock walls, an increase in shear stress because the channel becomes steeper (e.g., at a knickpoint), and a reduction in threshold stress as the stream crosses from sediment to a smooth rock bed. In Trout Beck all three are involved, with the third probably a consequence of the first two and giving a dramatic increase in transport capacity. However, some alluvial-to-bedrock transitions could involve only one or two of the possible causes. Rock-walled channels can be narrower than alluvial channels conveying the same water discharge because they can withstand higher near-bank shear stresses, but paired comparisons show exceptions to this tendency [*Wohl and David*, 2008]. Nor are bedrock reaches always steeper than adjacent alluvial reaches, though they often are at local outcrops of resistant rock or where bedrock is exposed because of differential uplift. Bedrock smoothness only becomes relevant once the rock is exposed, presumably through a downstream increase in shear stress, but it could then have a positive feedback effect. And not all bedrock reaches have smooth beds: some cross steeply dipping strata or have macroscopically rough beds because of potholes and other erosional features, and in such cases the local shear stress must be very high in order that transport capacity exceeds sediment supply.

The excess-stress methodology proposed by *Johnson* [2014] and employed in sections 4.5 and 5.2 above could be used to identify which combinations of step changes in width, slope, and bed roughness generate an increase in transport capacity from upstream alluvial channel to downstream bedrock channel. The calculations might, however, be sensitive to the poorly constrained choice of threshold stress for the rock bed, and in the long term the gradual incision of the bedrock reach could alter the initially imposed width and slope.

7. Conclusions

The presence of exposed rock in the bed of an otherwise alluvial channel implies a locally high transport capacity relative to sediment supply but leaves open the question of why this is and how the mobility of bed load has been enhanced. Our tracer experiment is one of the first attempts to investigate this in a field setting. By installing two identical sets of tracer stones, and estimating shear stresses in a series of short reaches of the channel, we were able to compare coarse sediment mobility on beds of contrasting character during the same flood events. The key results are as follows.

1. Tracers installed on exposed bedrock were far more mobile than elsewhere. This part of the channel experiences high mean shear stress, and threshold stress may be lower than elsewhere because of the smoothness of the rock bed.
2. Tracers were least mobile in the alluvial channel upstream from the gorge, which experiences relatively low shear stress. The difference in shear stress is sufficient to explain why natural bed load transport in the gorge is supply-limited.
3. The tracers that dispersed rapidly over exposed rock became preferentially stored near or in the next patch of partial sediment cover. This cover is exceptionally coarse, with many boulders, and tracers became concentrated first in the backwater zone immediately upstream of the sediment cover and then in that cover. We speculate that in situations where long-term incision supplies boulders to the river bed, they could act as nuclei for sediment cover and thus provide a negative feedback to incision rate.
4. Transport distances between successive surveys were higher during periods with higher peak discharge and increased approximately linearly with cumulative discharge above a threshold.
5. Tracer dispersion was neither size nor shape selective on exposed rock, but size selective on partial sediment cover and size and shape selective in the alluvial channel.
6. The behavior of the tracers was consistent with an excess shear stress framework for modeling bed load transport capacity.

Acknowledgments
This research was supported by a Durham University doctoral studentship to B.P.S., with additional fieldwork funding from a British Society for Geomorphology small grant. All authors contributed to planning the project, interpreting the results, and refining the paper. Fieldwork was done by B.P.S. with assistance from the other authors, technician Chris Longley, and numerous student helpers, notably Rosie Fewings and Alex Peters. R.I.F. drafted the paper. We thank Associate Editor Joel Johnson, reviewers Jens Turowski and Lindsay Olinde, and Editor John Buffington for their valuable comments and suggestions. The tracer-pebble data are available on request from R.I.F. (r.i.ferguson@durham.ac.uk) or R.A.H. (rebecca.hodge@durham.ac.uk).

References

Barry, J. J., J. M. Buffington, and J. G. King (2004), A general power equation for predicting bed load transport rates in gravel bed rivers, *Water Resour. Res.*, *40*, W10401, doi:10.1029/2004WR003190.

Beer, A. R., J. M. Turowski, B. Fritschi, and D. H. Rieke-Zapp (2015), Field instrumentation for high-resolution parallel monitoring of bedrock erosion and bedload transport, *Earth Surf. Processes Landforms*, *40*, 530–541.

Chatanantavet, P., and G. Parker (2008), Experimental study of bedrock channel alluviation under varied sediment supply and hydraulic conditions, *Water Resour. Res.*, *44*, W12446, doi:10.1029/2007WR006581.

Ferguson, R. I., and S. J. Wathen (1998), Tracer-pebble movement along a concave river profile: virtual velocity in relation to grain size and shear stress, *Water Resour. Res.*, *34*, 2031–2038, doi:10.1029/98WR01283.

Finnegan, N. J., L. S. Sklar, and T. K. Fuller (2007), Interplay of sediment supply, river incision, and channel morphology revealed by the transient evolution of an experimental bedrock channel, *J. Geophys. Res.*, *112*, F03511, doi:10.1029/2006JF000569.

Gilbert, G. K. (1877), Report on the geology of the Henry Mountains, 160 pp., U.S. Gov. Print. Off., Washington, D. C.

Goode, J. R., and E. Wohl (2010), Coarse sediment transport in a bedrock channel with complex bed topography, *Water Resour. Res.*, *46*, W11524, doi:10.1029/2009WR008135.

Hodge, R. A., and T. B. Hoey (2016), A Froude scale model of a bedrock-alluvial channel reach: 2. Sediment cover, *J. Geophys. Res. Earth Surf.*, *121*, 1597–1648, doi:10.1002/2015JF003709.

Hodge, R. A., T. B. Hoey, and L. S. Sklar (2011), Bed load transport in bedrock rivers: The role of sediment cover in grain entrainment, translation, and deposition, *J. Geophys. Res.*, *116*, F04028, doi:10.1029/2011JF002032.

Inoue, T., N. Izumi, Y. Shimizu, and G. Parker (2014), Interaction among alluvial cover, bed roughness, and incision rate in purely bedrock and alluvial-bedrock channel, *J. Geophys. Res. Earth Surf.*, *119*, 2123–2146, doi:10.1029/2014JF003133.

Johnson, G. A. L., and K. C. Dunham (1963), The Geology of Moor House, Monographs of the Nature Conservancy, Number Two, HMSO, London.

Johnson, J. P. (2014), A surface roughness model for predicting alluvial cover and bedload transport rate in bedrock channels, *J. Geophys. Res. Earth Surf.*, *119*, 2147–2173, doi:10.1029/2013JF003000.

Johnson, J. P., and K. X. Whipple (2010), Evaluating the controls of shear stress, sediment supply, alluvial cover, and channel morphology on experimental bedrock incision rate, *J. Geophys. Res.*, *115*, F02018, doi:10.1029/2009JF01335.

Lague, D. (2010), Reduction of long-term bedrock incision efficiency by short-term alluvial cover intermittency, *J. Geophys. Res.*, *115*, F02011, doi:10.1029/2008JF01210.

Meyer-Peter, E., and R. Müller (1948), Formulas for bed-load transport, 2nd Congress, International Association of Hydraulic Research, pp. 39-64, Stockholm.

Olinde, L., and J. P. L. Johnson (2015), Using RFID and accelerometer-embedded tracers to measure probabilities of bed load transport, step lengths, and rest times in a mountain stream, *Water Resour. Res.*, *51*, 7572–7589, doi:10.1002/2014WR016120.

Phillips, C. B., and D. J. Jerolmack (2014), Dynamics and mechanics of bed-load tracer particles, *Earth Surf. Dyn.*, *2*, 513–530.

Shobe, C. M., G. E. Tucker, and R. S. Anderson (2016), Hillslope-derived blocks retard river incision, *Geophys. Res. Lett.*, *43*, 5070–5078, doi:10.1002/2016GL069262.

Sklar, L. S., and W. E. Dietrich (2004), A mechanistic model for river incision into bedrock by saltating bed load, *Water Resour. Res.*, *40*, W06301, doi:10.1029/2003WR002496.

Thaler, E. A., and M. D. Covington (2016), The influence of sandstone caprock material on bedrock channel steepness within a technically passive setting: Buffalo National River basin, Arkansas, USA, *J. Geophys. Res. Earth Surf.*, *121*, 1635–1650, doi:10.1002/2015JF003771.

Turowski, J. M., D. Lague, and N. Hovius (2007), Cover effect in bedrock abrasion: A new derivation and its implications for the modeling of channel morphology, *J. Geophys. Res.*, *112*, F04006, doi:10.1029/2006JF000697.

Turowski, J. M., N. Hovius, A. Wilson, and M.-J. Horng (2008), Hydraulic geometry, river sediment and the definition of bedrock channels, *Geomorphology*, *99*, 26–38, doi:10.1016/j.geomorph.2007.10.001.

Whipple, K. X. (2004), Bedrock rivers and the geomorphology of active orogens, *Annu. Rev. Earth Planet. Sci.*, *32*, 151–185.

Wilcock, P. J., and J. C. Crowe (2003), Surface-based transport model for mixed-size sediment, *J. Hydraulic Eng.*, *129*, 120–128.

Wohl, E., and G. C. L. David (2008), Consistency of scaling relations among bedrock and alluvial channels, *J. Geophys. Res.*, *113*, F04013, doi:10.1029/2008JF000989.

Yager, E. M., J. W. Kirchner, and W. E. Dietrich (2007), Calculating bed load transport in steep boulder bed channels, *Water Resour. Res.*, *43*, W07418, doi:10.1029/2006WR005432.

Zhang, L., G. Parker, C. P. Stark, T. Inoue, E. Viparelli, X. Fu, and N. Izumi (2015), Macro-roughness model of bedrock-alluvial river morphodynamics, *Earth Surf. Dyn.*, *3*, 113–138, doi:10.5194/esurf-3-113-2015.